Cancer Investigation, 30:560–570, 2012
ISSN: 0735-7907 print / 1532-4192 online

DOI: 10.3109/07357907.2012.700985

informa
healthcare

CELLULAR AND MOLECULAR BIOLOGY

Buthionine Sulfoximine and 1,25-Dihydroxyvitamin D Induce Apoptosis in Breast Cancer Cells via Induction of Reactive Oxygen Species

Luciana P. Bohl,[1,*] Ana C. Liaudat,[1,*] Gabriela Picotto,[1] Ana M. Marchionatti,[1] Carmen J. Narvaez,[2] JoEllen Welsh,[2] Valeria A. Rodriguez,[1] and Nori G. Tolosa de Talamoni[1]

Laboratorio "Dr. Fernando Cañas," Bioquímica y Biología Molecular, Facultad de Ciencias Médicas, Universidad Nacional de Córdoba, Argentina,[1] GenNYsis Center for Excellence in Cancer Genomics, University at Albany, Albany, New York, USA[2]

Calcitriol or 1,25(OH)$_2$D$_3$ is a negative growth regulator of breast cancer cells. The aim of this study was to determine whether L-buthionine-S,R-sulfoximine, a glutathione-depleting drug, modifies the antiproliferative effects of 1,25(OH)$_2$D$_3$ on MCF-7 cells. For comparison, we included studies in MCF-7 cells selected for vitamin D resistance and in human mammary epithelial cells transformed with SV40 and *ras*. Our data indicate that L-buthionine-S,R-sulfoximine enhances the growth inhibition of 1,25(OH)$_2$D$_3$ in all transformed breast cell lines. This effect is mediated by ROS leading to apoptosis. In conclusion, BSO alters redox state and sensitizes breast cancer cells to 1,25(OH)$_2$D$_3$-mediated apoptosis.

Keywords: 1,25 (OH)$_2$D$_3$ or calcitriol, BSO, Breast cancer cell, Apoptosis, ROS, GSH

INTRODUCTION

Epidemiological studies have suggested that high levels of serum 25OHD$_3$, which reflects an individual's vitamin D status, is associated with reduced risk of breast cancer development and progression (1–3). Furthermore, studies in animal models of breast cancer, including human xenograft experiments, have shown that vitamin D reduces both initiation and progression of breast tumors (4–6). Although activation of the vitamin D receptor by 1,25(OH)$_2$D$_3$, the biologically active metabolite of vitamin D, is known to trigger antiproliferative and prodifferentiating effects in a wide variety of malignant and normal tissues (7, 8), the specific molecular mechanisms that mediate these effects have yet to be clarified. In addition, sensitivity to vitamin D is reduced as cancer progresses and upon chronic exposure to 1,25(OH)$_2$D$_3$. Furthermore, the development of vitamin D-based strategies for breast cancer prevention or treatment has been limited by calcemic side effects (8). Although a number of vitamin D analogs have been synthesized that display reduced calcemic effects relative to 1,25(OH)$_2$D$_3$, the therapeutic window for these compounds remains small. For this reason, agents that synergize cells to the anticancer effects of vitamin D have been sought, with the expectation that combination therapies could improve therapeutic efficacy while reducing toxicity. A few small clinical trials have employed this approach, combining vitamin D therapies with dexamethasone or taxol derivatives, with some promising results (9–12). Although breast cancer is a common malignancy and is a major cause of cancer death in women, few agents that enhance the responsiveness of breast cancer cells to vitamin D have been identified to date.

1,25(OH)$_2$D$_3$ inhibits cellular proliferation by blocking the G_1 to S transition in association with induction of cyclin-dependent kinase inhibitors p21 or p27, dephosphorylation of the retinoblastoma protein, and decreased activity of various cyclins (A_1, D_1, D_3, and E_1) (13–15). Apoptosis induction by 1,25(OH)$_2$D$_3$ in breast cancer cells has been linked to changes in effector and inflammatory caspases and Ca^{2+} release from intracellular stores leading to calpain activation (16, 17). 1,25(OH)$_2$D$_3$ modulates genes required for maintenance of redox status, such as thioredoxin reductases, alters the subcellular localization and activity of thioredoxin-1, and induces accumulation of reactive oxygen species (ROS) in MCF-7 breast cancer cells (18–21). Furthermore, thioredoxin-1 activity was higher in MCF-7 cells selected for resistance to 1,25(OH)$_2$D$_3$-mediated apoptosis (22). Taken together, these findings indicate that multiple pathways contribute to the antiproliferative and apoptotic effects of 1,25(OH)$_2$D$_3$, including several that regulate cellular redox state.

Overexpression of the antioxidant glutathione (GSH) has been observed in primary breast tumors and in lymph node metastases (23). *In vitro*, increased intracellular GSH induces resistance of breast cancer cells to cytotoxic agents whereas GSH-depleting drugs potentiate the effect of anticancer drugs (24–26). In previous studies, we demonstrated

*Have contributed equally.

Correspondence to: Prof. Dr. Nori Tolosa de Talamoni, Cátedra de Bioquímica y Biología Molecular, Facultad de Ciencias Médicas, Universidad Nacional de Córdoba, Pabellón Argentina, 2do. Piso, Ciudad Universitaria, 5014 Córdoba, Argentina, email: ntolosatalamoni@yahoo.com.ar; ntolosa@biomed.fcm.unc.edu.ar

that menadione (MEN), an agent that reduces intracellular GSH due to the redox cycle of the quinone metabolism (27), potentiates the effects of $1,25(OH)_2D_3$ on MCF-7 cell growth in association with enhanced oxidative stress. Because MEN has additional cellular effects including vitamin K activity, in these follow-up studies we sought to determine whether agents that specifically induce GSH depletion would sensitize breast cancer cells to $1,25(OH)_2D_3$. L-buthionine-S,R-sulfoximine (BSO) is a selective inhibitor of gamma glutamyl cysteine ligase, which catalyzes the rate limiting step of GSH synthesis. BSO has been shown to deplete intracellular GSH and sensitize tumor cells to apoptosis induced by standard chemotherapeutic agents (28–31). Lewis-Wambi *et al*. (25) demonstrated that BSO sensitized antihormonal-resistant MCF-7:2A cells to estradiol-induced apoptosis. Based on these previous observations, the aim of the current study was to determine whether BSO modified the effects of $1,25(OH)_2D_3$ on MCF-7 cell growth or apoptosis *in vitro*. For comparison purposes, we included studies in MCF-7 cells selected for vitamin D resistance and in human mammary epithelial cells transformed with SV40 and *ras*. Our data indicate that BSO significantly enhances the growth inhibitory effects of $1,25(OH)_2D_3$ in all transformed breast cell lines tested, providing proof of principle that BSO, which is less toxic than menadione, might represent a more suitable drug for combination treatment with vitamin D analogs in breast cancer patients.

MATERIALS AND METHODS

Chemicals

Dulbecco's Modified Eagle Medium (DMEM), phosphate buffered saline (PBS), and trypsin-EDTA (0.05%) were purchased from Gibco (Invitrogen, Grand Island, NY, USA). Fetal bovine serum (FBS) was from Natocor (Carlos Paz, Argentina). BSO (L-buthionine-S,R-sulfoximine) was obtained from Sigma (St. Louis, MO, USA). $1,25(OH)_2D_3$ was a generous gift from F. Hoffmann-La Roche Ltd. (Basel, Switzerland). All other reagents were of analytical grade.

Cells and cell culture

Human breast cancer MCF-7 and vitamin D-resistant MCF-7 ($MCF\text{-}7^{DR}$) cells (16) were maintained in DMEM supplemented with FBS (5%), penicillin (100 U/mL), and streptomycin (100 μg/mL) at 37°C and were subcultured once a week. Human breast cancer cells generated by oncogenic transformation of primary mammary epithelial cells (HMLER cells, obtained through the introduction of hTERT, SV40 large T antigen, and H-*ras*-V12, provided by Dr. R. A. Weinberg, MIT, Cambridge, MA) (32) were cultured in Medium 171 supplemented with mammary epithelial growth supplements (Invitrogen) at 37°C and subcultured twice a week. For experiments, cells were plated in 10-cm plates, grown in complete media for 24 hr and treated with $1,25(OH)_2D_3$ in the presence or absence of BSO for different times at the indicated concentrations. Cells treated with vehicle alone (ethanol, less than 0.05%) were included in all assays.

Cell growth assay

Adherent cell number was evaluated as previously described (16). Briefly, cells seeded at 2×10^3 cells/well in 24-well plates were allowed to attach for 24 hr and then exposed to $1,25(OH)_2D_3$, with or without BSO, or vehicle alone for the indicated times. Cells were then fixed with 1% glutaraldehyde, incubated with 0.1% crystal violet, destained with H_2O, and solubilized with Triton X-100 (0.2%). Absorbance, which is proportional to adherent cell number under the conditions used, was measured at 562 nm (minus background at 630 nm). Data represent mean ± standard error of 4–6 wells per treatment and are representative of three replicate experiments.

Evaluation of apoptosis and morphology

MCF-7 cells were grown on Lab-Tek II chamber slides (Fisher Scientific, Rochester, NY, USA) and exposed to $1,25(OH)_2D_3$ in the presence or absence of BSO, or ethanol vehicle, for 96 hr. Cells were fixed in 4% formaldehyde, permeabilized in ice-cold methanol, and blocked overnight with PBS/1% BSA. For detection of cytochrome c, cells were incubated with mouse monoclonal antibody to cytochrome c (BD PharMingen Biosciences, San Jose, CA, USA) for 3 hr at 37°C. Slides were washed with PBS followed by incubation for 1 hr with anti-mouse secondary antibody conjugated to ALEXA-488 (Molecular Probes, Eugene, OR, USA). Fluorescence was counted in nuclei and entire cells by using the Image J 1.45S (NIH) software. The fluorescence analysis of data was accomplished following a procedure previously described (33) and later the nuclei/cytosol fluorescence ratios were calculated. Slides were incubated for 15 min at room temperature with 1 μg/mL Hoechst 33258 (Sigma), washed with PBS, rinsed with distilled H_2O, and coverslips were applied with an antifade reagent. For detection of DNA strand breaks, the *in situ* cell death detection kit (Boehringer Mannheim, Germany) was used according to the manufacturer's instructions on cells grown, fixed and permeabilized as described earlier. This assay labels individual cells undergoing apoptosis by terminal transferase-mediated addition of fluorescein dUTP at DNA strand breaks. Phase contrast and fluorescence images were obtained using an Olympus AX70 microscope equipped with a Spot RT digital camera (Sterling Heights, MI, USA). Caspase assay for *in situ* apoptosis was performed in MCF-7 cells exposed to $1,25(OH)_2D_3$ in the presence or absence of BSO, or ethanol vehicle, for 72 or 96 hr. Positive controls for apoptosis were accomplished in MCF-7 cells treated with 1 ng/mL TNF-alpha (Sigma-Aldrich, St. Louis, MO, USA). CaspACE FITC-VAD-FMK In Situ Marker (Promega, Madison, WI, USA) was used according to the manufacturer's protocol. Pictures were undertaken with a Leica DMI6000 microscope with TCS SP5 confocal laser scanner (Leica Microsystems Inc., Buffalo Grove, IL, USA). Fluorescence values were acquired and analyzed by using an IN Cell Analyzer 1000 (Amersham Biosciences, Piscataway, NJ, USA).

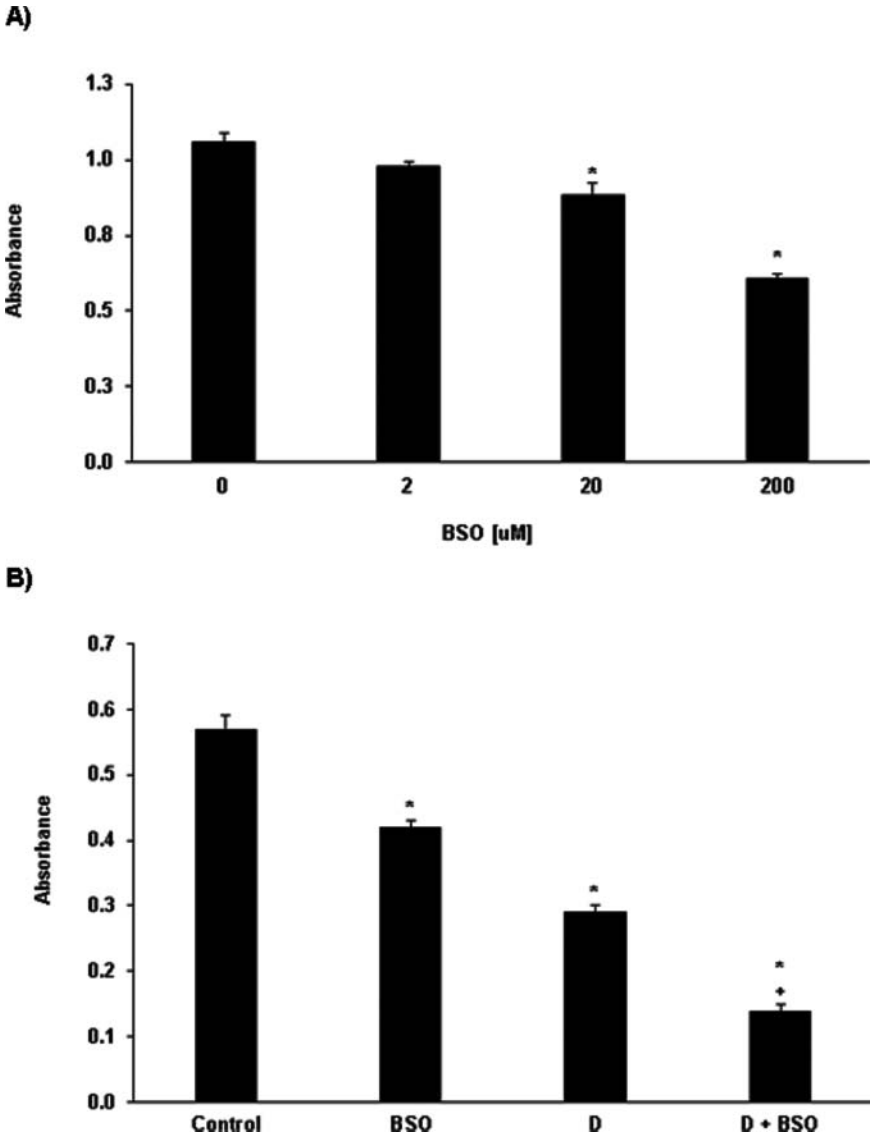

Figure 1. Cell growth of MCF-7 cells treated with BSO and/or $1,25(OH)_2D_3$ (D). (A) MCF-7 cells were treated with 2, 20, or 200 μM BSO for 96 hr. (B) MCF-7 cells were treated with 20 μM BSO and/or 100 nM $1,25(OH)_2D_3$ for 96 hr. Values represent means ±SE. $^*p < .05$ versus Control, $+p < .05$ versus 20 μM BSO and 100 nM $1,25(OH)_2D_3$.

Flow cytometry

For cell cycle analysis, cells were harvested by trypsinization, collected by centrifugation, fixed in 100% ethanol at –20°C, and incubated with propidium iodide (5 μg/mL) and RNAse (0.015 U/mL) in PBS for 20 min (34). Cell cycle analysis was performed on BD FACSCanto™ II Flow Cytometer (BD Biosciences, San Jose, CA, USA). PI was analyzed on 564–606 nm band pass filter. Data were modeled using the FlowJo 7.6.4 software (Tree Star, Ashland, OR, USA).

For measurement of ROS production, cells were collected by trypsinization and pelleted by centrifugation. Cell suspensions (5×10^5 cells) were incubated with 4 μM hydroethidine (HE, Molecular Probes, Invitrogen) in PBS for 15 min at 37°C. Conversion of HE to ethidium by superoxide anion was analyzed with an Epics XL Flow Cytometer (Coulter Corp., Miami, USA) on FL3 using a 620 nm band pass filter. Data were analyzed using MULTIPLUS AV analysis software (Phoenix Flow Systems, Inc., San Diego, CA, USA) (16).

Determination of total GSH

After treatment, cells were washed and resuspended in PBS buffer plus 1 mM PMSF, 1 mM NaF, 1% Triton X-100, and homogenized at 4°C. Homogenates were cleared by centrifugation ($15{,}000 \times g$) for 30 min at 4°C, and supernatants were used to evaluate GSH content using the glutathione disulfide reductase-5,5′-dithiobis (2-nitrobenzoate) recycling procedure (35). Protein concentrations were determined using purified serum albumin as standard by Bradford assay (36).

Statistical analysis

Data were evaluated by one-way analysis of variance (ANOVA) and Bonferroni *post hoc* test. Differences were considered significant at $p < .05$ using SPSS software for Windows Release 8.0.0 Standard Version (SPSS Inc., Chicago, IL, USA).

RESULTS

Effects of 1,25(OH)$_2$D$_3$ and BSO on cell number and cell cycle

We first examined the effects of BSO alone on growth of MCF-7 cell cultures. After 96 hr, dose-dependent growth inhibition was observed, with significantly reduced cell density at concentrations of 20 μM BSO or higher (Figure 1A). We then examined the effects of 20 μM BSO in the presence of 100 nM 1,25(OH)$_2$D$_3$, a dose known to inhibit MCF-7 cell growth in this time frame. As shown in Figure 1(B), 100 nM 1,25(OH)$_2$D$_3$ exerted a more pronounced inhibitory effect on MCF-7 cell growth than 20 μM BSO, and an additive effect was observed in cells cotreated with both agents. While BSO at 100 μM was more potent as a single agent, the additive effect of 100 μM BSO and 100 nM 1,25(OH)$_2$D$_3$ was not significantly different than that observed with 20 μM BSO and 100 nM 1,25(OH)$_2$D$_3$ (data not shown). No significant changes in cell density were observed at shorter exposure times for either agent alone. Since 20 μM BSO was the lowest effective dose in growth inhibition, this dose was used for the remaining experiments.

Flow cytometry was utilized to determine whether cell cycle arrest preceded the reduction in cell density induced by BSO, and whether sensitization of MCF-7 cells to the effect of 1,25(OH)$_2$D$_3$ was associated with changes in cell cycle kinetics. While no effects of 20 μM BSO alone on cell cycle were observed, an increased percentage of cells in G_1 phase and a decreased percentage in S phase was observed with 100 nM 1,25(OH)$_2$D$_3$ (Table 1). Simultaneous treatment with 100 nM 1,25(OH)$_2$D$_3$ and 20 μM BSO had no additional effects on cell cycle kinetics at 72 hr or 96 hr (data not shown). None of the treatments altered the percentage of cells in G_2.

Table 1. Effects of BSO and 1,25(OH)$_2$D$_3$ (D) on Cell Cycle Distribution in MCF-7 Cells

	G_1	S	G_2
Control	63 ± 1	26 ± 1	10 ± 2
BSO	63 ± 1	25 ± 1	11 ± 1
D	$70 \pm 1^*$	$18 \pm 2^*$	10 ± 2
D + BSO	$68 \pm 1^*$	$19 \pm 1^*$	11 ± 1

Note: Cells were treated with vehicle (ethanol), 20 μM BSO, 100 nM 1,25(OH)$_2$D$_3$, or both drugs for 72 hr. Cell percentages at each cell cycle phase were determined by flow cytometry.
Values represent means $\pm$ SE.
$^*p < .05$ versus Control.

Effects of 1,25(OH)$_2$D$_3$ and BSO on apoptosis

To evaluate the possibility that apoptosis was induced in MCF-7 cells treated with BSO alone or in combination with 1,25(OH)$_2$D$_3$, cell and nuclear morphology was analyzed after 96 hr treatment (Figure 2). No morphological evidence of apoptosis was observed in cells treated with 20 μM BSO. In contrast, cells treated with 100 nM 1,25(OH)$_2$D$_3$ alone or in combination with 20 μM BSO displayed morphological features of apoptosis including cell shrinkage, condensed chromatin, withdrawal of cell-to-cell contacts, and loss of adherence (Panel A). Moreover, apoptotic bodies typical of late apoptosis were detected with Hoechst nuclear staining in cells treated with 1,25(OH)$_2$D$_3$ or both agents (Panel B). DNA fragmentation was specifically determined by terminal dUTP nick end labeling (TUNEL) staining (Panel C). In cultures treated with 1,25(OH)$_2$D$_3$ or both agents, TUNEL-positive cells were more prevalent relative to control or BSO-treated cultures. Since cytochrome c translocation from mitochondria to cytoplasm and nucleus is a trait of the intrinsic apoptotic pathway, we also measured

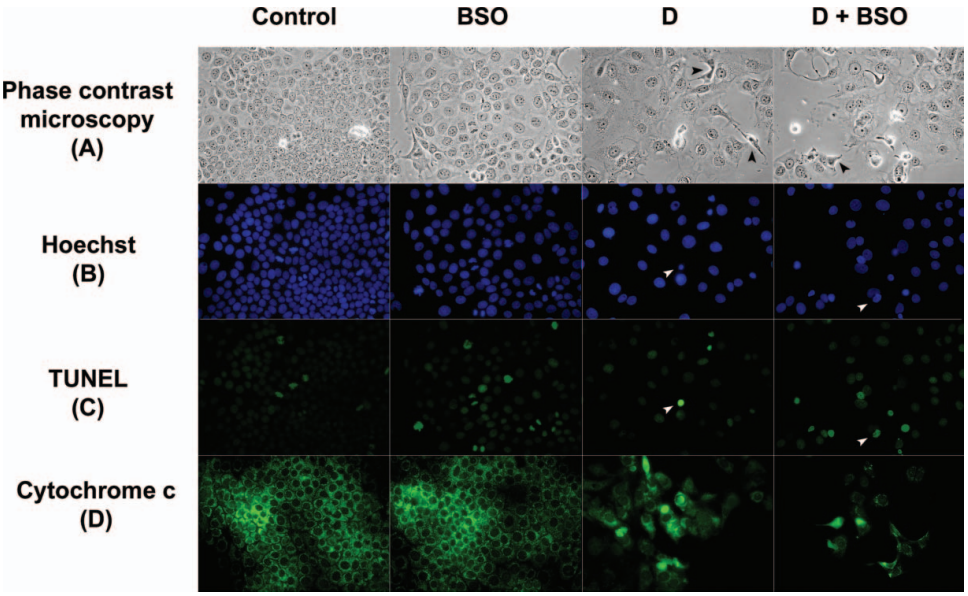

Figure 2. Effects of BSO and 1,25(OH)$_2$D$_3$ (D) on MCF-7 cell morphology, TUNEL and cytochrome c staining. MCF-7 cells were treated with vehicle (ethanol), 20 μM BSO, 100 nM 1,25(OH)$_2$D$_3$ or both drugs for 96 hr. (A) Phase contrast microscopy (magnification, 200×) shows apoptotic cells (arrows). (B) Hoechst fluorescence microscopy shows typical apoptotic bodies (arrows). (C) Fluorescence microscopy of TUNEL staining. Positive cells are pointed with arrows. (D) Fluorescence microscopy of MCF-7 immunostained with cytochrome c antibody. The same field was used to acquire (A) phase contrast, (B) Hoechst, and (C) TUNEL staining images.

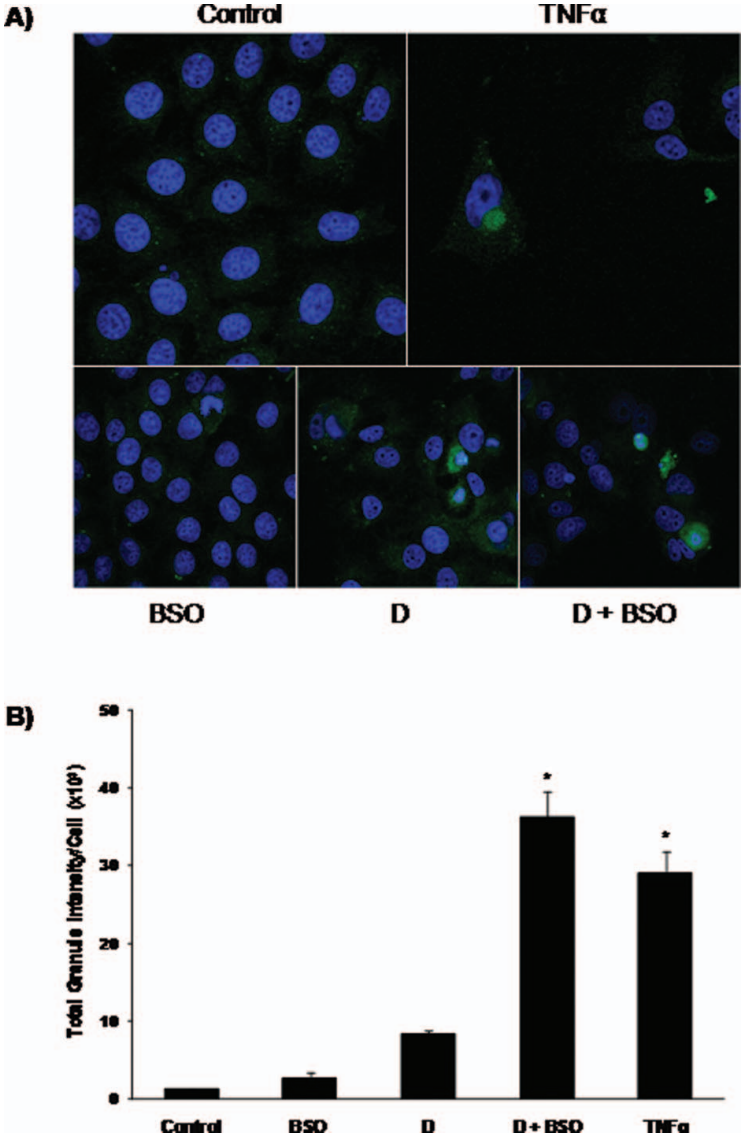

Figure 3. Effects of BSO and $1,25(OH)_2D_3$ (D) on caspase activation *in situ* in MCF-7 cells. Cells were incubated for 72 hr with 20 μM BSO and/or 100 nM $1,25(OH)_2D_3$. Positive controls were performed by using 1 ng/mL TNF-alpfa. Caspase activation was determined by using CaspACE FITC-VAD-FMK In Situ Marker kit. (A) Pictures were taken by using a confocal microscope. (B) Fluorescence data were acquired with an IN Cell Analyzer and are expressed in total granule intensity/ cell ($\times 10^3$). Values represent means ± SE. * $p < .05$ versus Control, BSO, and D.

the nuclei/cytoplasm ratio of fluorescent cytochrome c. As shown in Figure 2, Panel D, cytochrome c staining was restricted to the cytoplasm (where mitochondria are localized) in both control and BSO-treated cells. In contrast, cells treated with $1,25(OH)_2D_3$ or $1,25(OH)_2D_3$ plus BSO displayed cytochrome c staining not only in the cytoplasm but also in nuclei (3-fold enhancement in the nuclei/cytoplasm ratio in cells treated with $1,25(OH)_2D_3$, and 10-fold in cells treated with $1,25(OH)_2D_3$ plus BSO), an indication of cytochrome c translocation out of the mitochondria. Caspase activation *in situ* revealed that either BSO or $1,25(OH)_2D_3$ for 72 hr produced the same response of MCF-7 cells treated with vehicle, whereas $1,25(OH)_2D_3$ plus BSO increased significantly the enzymatic activation. TNF-alpha (1 ng/mL), a known apoptotic inducer, also produced caspase activation in MCF-7 cells causing a similar response to that obtained with the combined treatment (Figure 3). After 96 hr of treatment, enhancement of caspase activation *in situ* was caused either by the combined treatment or by $1,25(OH)_2D_3$ alone. Total granule fluorescence intensity/cell was as follows (means ± E.S.): Control ($4.49 \times 10^3 \pm 2.19 \times 10^3$), BSO ($3.81 \times 10^{3*} \pm 0.54 \times 10^3$, $^*p < .05$ vs. $1,25(OH)_2D_3$ or $1,25(OH)_2D_3$ plus BSO), $1,25(OH)_2D_3$ ($95.62 \times 10^{3\dagger} \pm 7.39 \times 10^3$, $^\dagger p < .05$ vs. Control, BSO, and $1,25(OH)_2D_3$ plus BSO), $1,25(OH)_2D_3$ plus BSO ($210.50 \times 10^{3\P} \pm 6.43 \times 10^3$, $^\P p < .05$ vs. Control, BSO, and $1,25(OH)_2D_3$).

Effects of $1,25(OH)_2D_3$ and BSO on cellular redox status

To assess whether oxidative stress was associated with apoptosis triggered by either $1,25(OH)_2D_3$ or the combined treatment, we determined total GSH content and ROS generation. As expected, treatment with BSO for 96 hr significantly

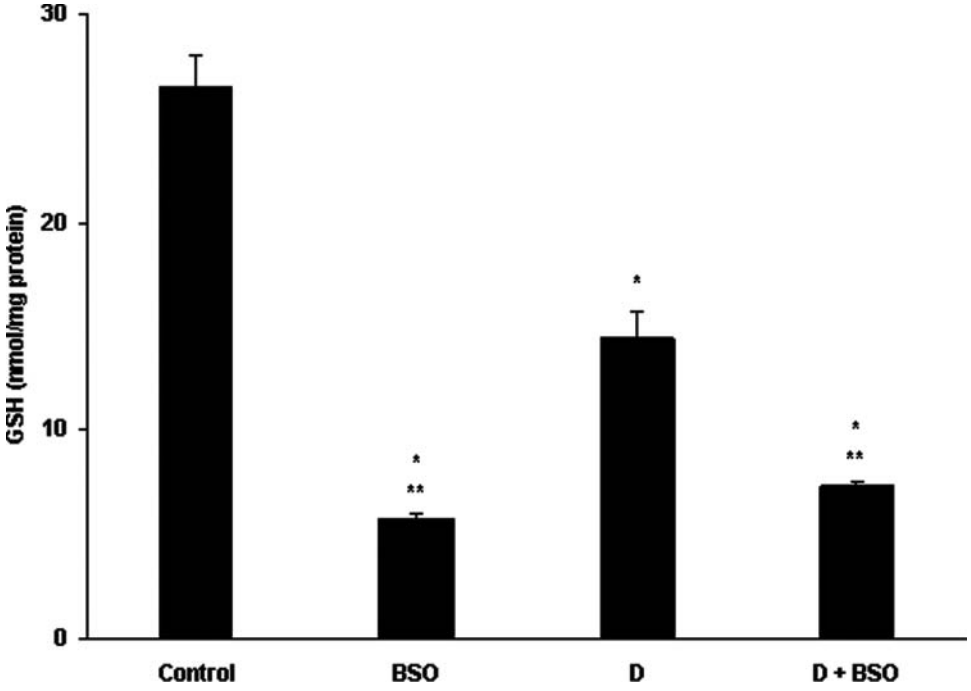

Figure 4. GSH content of MCF-7 cells in response to 1,25(OH)2D3 (D) and/or BSO. Cells were incubated for 96 hr with 20 μM BSO and/or 100 nM $1,25(OH)_2D_3$. Values represent means ± SE. $^{*}p < .05$ versus Control; $^{**}p < .05$ versus $1,25(OH)_2D_3$.

reduced total GSH content (Figure 4). $1,25(OH)_2D_3$ treatment alone also significantly reduced total GSH content, but to a lesser extent than BSO. Interestingly, GSH content of cells treated with both $1,25(OH)_2D_3$ and BSO had intermediate GSH content, with no evidence of an additive effect of the two agents. We also measured ROS production by flow cytometry (Figure 5) and found that $1,25(OH)_2D_3$ treatment significantly increased ROS but BSO treatment alone had minimal effects (29.6% vs. 4.7% ROS positive cells, respectively). This effect was further enhanced when both drugs were administered simultaneously (42.8% ROS positive cells).

Effects of $1,25(OH)_2D_3$ and BSO on additional cell lines

To determine whether BSO could affect growth of vitamin D-resistant breast cancer cells, we used MCF-7^{DR} cells, a variant of MCF-7 cells which were selected for resistance to $1,25(OH)_2D_3$. As expected, 100 nM $1,25(OH)_2D_3$ had minimal effects on growth of MCF-7^{DR} cultures compared to the MCF-7 parental cells (i.e., Figure 1 vs. Figure 6A). BSO alone produced a small antiproliferative effect in a dose-dependent manner (data not shown). Combined treatment with $1,25(OH)_2D_3$ and BSO further reduced cell numbers in MCF-7^{DR} cultures, however the response was still much lower than that observed in the parental MCF-7 cells (Figure 6A).

Since MCF-7 cells represent a well-differentiated estrogen receptor positive breast cancer cell line, it was of interest to test whether similar effects of $1,25(OH)_2D_3$ and BSO would be retained in an estrogen receptor negative transformed breast cell line. We utilized HMLER cells, which were created via retroviral transduction of hTERT, SV40 large T antigen and oncogenic *ras* into normal human mammary epithelial cells (32). HMLER cells are tumorigenic in nude mice but lack expression of estrogen and progesterone receptors and do not demonstrate amplification at the HER2 genomic locus, thus, they represent a model of triple negative breast cancers (32). As shown in Figure 6(B), HMLER cells were more sensitive to BSO and less sensitive to $1,25(OH)_2D_3$ than MCF-7 cells (Figure 1). Similar to MCF-7 cells, however, maximal growth reduction was achieved when HMLER cells were treated with both agents (Figure 6B).

DISCUSSION

The present data demonstrate that the GSH depleting agent BSO sensitizes MCF-7 breast cancer cells to the antitumor effects of the vitamin D receptor ligand $1,25(OH)_2D_3$. We confirmed that the growth inhibitory effect of 100 nM $1,25(OH)_2D_3$ in MCF-7 cells treated for 96 hr is approximately 50% (15, 16, 27) and showed that when cotreated with 20 μM BSO, growth reduction of approximately 75% is achieved. To explore the mechanisms of growth inhibition under these conditions, we documented the independent and combined effects of these agents on GSH content, ROS, apoptosis, and cell cycle. BSO alone dramatically decreased intracellular GSH content and had minimal effects on cell cycle, ROS production, or apoptosis. In contrast, $1,25(OH)_2D_3$ alone had less effect on GSH content but induced cell cycle arrest in G_0/G_1, enhanced ROS production, and triggered apoptosis via cytochrome c release and caspase activation. Cells treated with both BSO and $1,25(OH)_2D_3$ exhibited enhanced ROS production and apoptosis, but no further depletion of GSH than BSO treatment alone, and no further effects on cell cycle than $1,25(OH)_2D_3$ alone. Collectively, these data indicate that the enhanced effect of combination

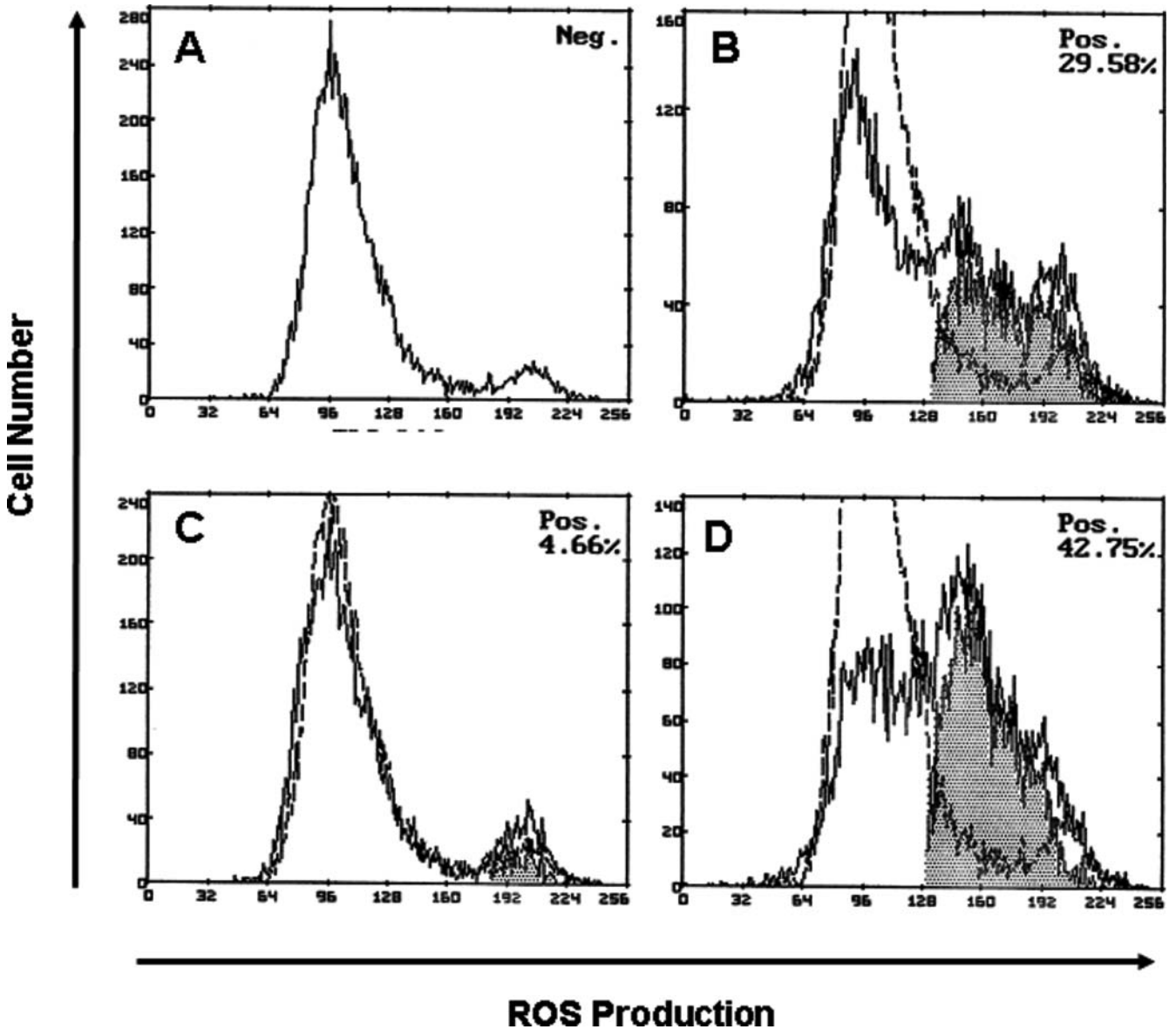

Figure 5. Effects of $1,25(OH)_2D_3$ (D) and/or BSO on ROS production in MCF-7 cells. Cells were treated with 20 μM BSO and/or 100 nM $1,25(OH)_2D_3$ for 96 hr. ROS production was analyzed by flow cytometry. Numbers in upper right corner of each panel indicate the percentage of positive cells after negative subtraction of data obtained with vehicle-treated cells: (A) cells treated with vehicle; (B) cells treated with $1,25(OH)_2D_3$; (C) cells treated with BSO; (D) cells treated with $1,25(OH)_2D_3$ and BSO. The figure is representative from at least four independent experiments.

treatment in reducing growth of MCF-7 cultures is mediated via increased ROS production leading to apoptosis rather than GSH depletion or cell cycle arrest.

Relationships between GSH, ROS, and apoptosis have been explored in several studies. Koren *et al*. (37) demonstrated that the effect of BSO on GSH content of MCF-7 cells is dose-dependent and saturates at a concentration of 20 μM, the dose used in these studies. This could explain, at least in part, why the combined treatment did not further decrease GSH content as compared to BSO alone. Under the conditions used, depletion of GSH by BSO alone was not sufficient to trigger significant ROS accumulation. Regardless, synergistic effects of BSO and $1,25(OH)_2D_3$ on ROS production were clearly observed in association with apoptosis after 96 hr treatment. Depending on the cellular context, ROS can act both as second messengers in intracellular signaling cascades and as inducers of cell death (38). High levels of ROS overload the capacity of superoxide dismutase and other antioxidants, leading to sustained oxidative stress eventually causing cell death (39). In our studies, decrease of GSH content alone (as with BSO treatment), which did not significantly enhance ROS, did not trigger apoptosis. The lack of effect of BSO alone on apoptosis was previously reported in lung cancer Calu-6 cells (40) and in metastatic breast cancer cells (25), although BSO was shown to trigger apoptosis in several neuroblastoma cell lines (39). These discrepancies may be related to culture conditions, since the effect of GSH on cell viability was shown to be density-dependent in Ht22 cells derived from mouse hippocampus (41). Differences in BSO sensitivity, intracellular GSH content, or the

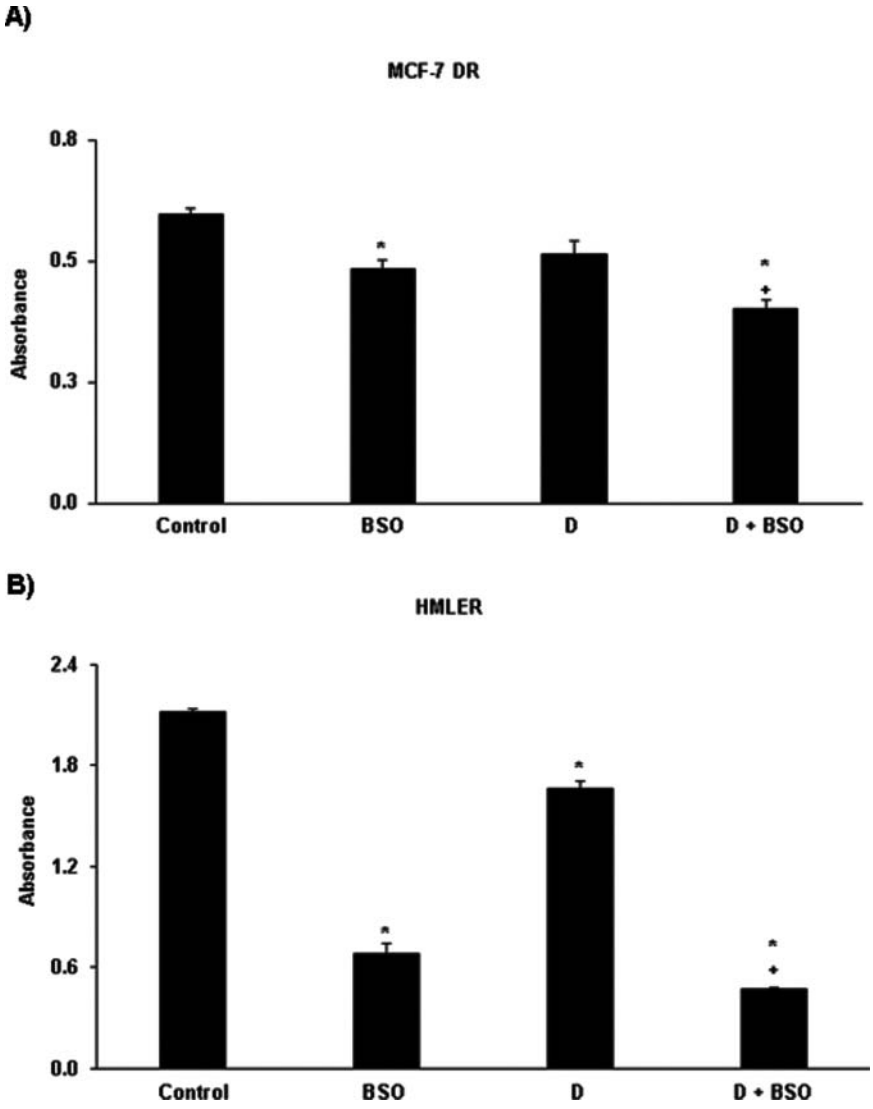

Figure 6. Cell growth of MCF-7 DR (A) and HMLER (B) cells treated with BSO and/or 1,25(OH)2D3 (D). Cells were treated with 20 μM BSO and/or 100 nM $1,25(OH)_2D_3$ for 96 hr. Values represent means ± SE. $^*p < .05$ versus Control, $+p < .05$ versus 20 μM BSO and 100 nM $1,25(OH)_2D_3$.

downstream cascade to GSH depletion might also explain the variability in the apoptotic responses of cancer cells to BSO.

Apoptosis in response to either $1,25(OH)_2D_3$ or the combination treatment was associated with the release of cytochrome c from mitochondria reaching the nuclei, indicating involvement of the intrinsic pathway. Since ROS is mainly generated as a subproduct of electron transport in the mitochondria (37), mitochondrial dysfunction might be induced by the combined treatment secondary to oxidative stress. ROS production has been described as an early event in several apoptotic models (42, 43), and in MCF-7 cells treated with $1,25(OH)_2D_3$, ROS production and cytochrome c release occur before the appearance of apoptotic morphology (16). It has been proposed that ROS open the mitochondrial permeability transition pore and/or dissipate the mitochondrial membrane permeabilization, leading to release of apoptogenic factors including cytochrome c (44). ROS have also been shown to downregulate bcl-2 expression, which can further sensitize cells to apoptotic death (45). Thus, there are many potential mechanisms by which the enhanced ROS generated by combined treatment with $1,25(OH)_2D_3$ and BSO could trigger apoptosis.

Our data also demonstrate that the cooperative effect of BSO and $1,25(OH)_2D_3$ was retained in MCF-7^{DR} cells, a variant of MCF-7 cells, which were selected for resistance to $1,25(OH)_2D_3$. However, the magnitude of growth inhibition by the combination treatment was much lower in MCF-7^{DR} cells than in parental MCF-7 cells (33% in MCF-7^{DR} cells vs. 73% in MCF-7 cells). MCF-7^{DR} cells were also less sensitive to BSO-mediated growth inhibition. Genomic and proteomic approaches have demonstrated that multiple growth factor signaling pathways and apoptotic regulators are altered in $1,25(OH)_2D_3$-resistant MCF-7 cell lines (21, 22) including several involved in redox control such as thioredoxin. These changes might underlie the reduced sensitivity of the vitamin D-resistant cells to BSO. In addition, treatment with BSO in the presence of $1,25(OH)_2D_3$ might sufficiently alter

redox status to circumvent these altered pathways and partially overcome the resistance phenotype. In support of this concept, we previously showed that combining menadione, another GSH lowering agent, with $1,25(OH)_2D_3$ had similar effects on MCF-7^{DR} cells (27).

Of particular interest with respect to advanced breast cancer, we also demonstrated that the combination treatment enhanced the growth inhibitory effects of $1,25(OH)_2D_3$ in HMLER cells, a model of triple negative disease. Although these cells are fairly unresponsive to $1,25(OH)_2D_3$ due to downregulation of the vitamin D receptor during transformation (46), they were highly responsive to BSO (70% growth inhibition in HMLER vs. 20% in MCF-7). Furthermore, combination therapy with BSO and $1,25(OH)_2D_3$ was equally effective in HMLER and MCF-7 cells.

In summary, our data indicate that the GSH depleting agent BSO and the VDR agonist $1,25(OH)_2D_3$ independently trigger growth inhibition in breast cancer cells. Furthermore, both estrogen receptor negative and positive cell lines exhibited similar growth inhibition when treated with the two agents in combination. The identification of new agents for the treatment of breast cancer is clearly of interest since current therapies are often limited by short-term efficacy due to the emergence of drug resistance. Although vitamin D-based drugs have been proposed as potential agents for breast cancer based on preclinical animal models, their efficacy has not been demonstrated in the clinic, in part due to the narrow therapeutic window for $1,25(OH)_2D_3$ and its synthetic analogs (8). Our studies indicate that reduction of cellular GSH content may be one strategy to enhance the efficacy of $1,25(OH)_2D_3$ and vitamin D analogs as anticancer agents. The synergistic effects of $1,25(OH)_2D_3$ and BSO could diminish the adverse effects of high doses of calcitriol, especially related to calcium metabolism (8). The concentration of BSO used in our study is clinically achievable (24) and it has been employed safely in several clinical trials (24, 47, 48) or undergoing clinical studies (49, 50). Future preclinical studies exploring the anticancer properties of $1,25(OH)_2D_3$ and BSO could open new avenues for the treatment of human breast cancer.

ACKNOWLEDGMENTS

The authors want to thank Mrs. Angela Perrin from Hoffmann-La Roche Ltd., Basel, Switzerland.

DECLARATION OF INTERESTS

Part of this work was accomplished by Prof. Dr. Nori Tolosa de Talamoni as a Fulbright Award recipient. The exchange of the investigators (Dr. N.T. de T and Dr. J.W.) was funded by the International Collaboration between CONICET and the National Science Foundation. Prof. Dr. Nori Tolosa de Talamoni and Dr. Gabriela Picotto are members of the Investigator Career from CONICET. Luciana P. Bohl, Ana C. Liaudat, and Valeria Rodríguez are recipients of CONICET fellowships. Work in Prof. Dr. Tolosa de Talamoni's lab was supported by Grants from CONICET (PIP 2010–12), Ministerio de Ciencia y Tecnología de la Provincia de Cordoba (PID 2008), Instituto Nacional del Cancer (Argentina), and SECYT (UNC), Argentina. Work in Dr. Welsh's lab was supported by grants from NIH (CA69700 and CA144963). The authors report no conflicts of interest. The authors alone are responsible for the content and writing of the article.

ABBREVIATIONS

BSO	L-buthionine-S,R-sulfoximine
GSH	glutathione
ROS	reactive oxygen species
MCF-7^{DR}	human breast cancer vitamin D resistant cells
HMLER	human breast cancer cells generated by oncogenic transformation of primary mammary epithelial cells
$25OHD_3$	25 hydroxyvitamin D_3
VDR	vitamin D receptor
MEN	menadione
DMEM	Dulbecco's Modified Eagle Medium
PBS	phosphate buffered saline
FBS	fetal bovine serum
TUNEL	terminal dUTP nick end labeling
HE	hydroethidine
PMSF	phenyl methanesulphonyl fluoride

REFERENCES

1. Krishnan AV, Feldman D. Mechanisms of the anti-cancer and anti-inflammatory actions of vitamin D. Annu Rev Pharmacol Toxicol 2011;51:311–336.
2. Welsh J. Cellular and molecular effects of vitamin D on carcinogenesis. Arch Biochem Biophys 2011;523:107–114.
3. Yin L, Grandi N, Raum E, Haug U, Arndt V, Brenner H. Meta-analysis: serum vitamin D and breast cancer risk. Eur J Cancer 2010;46:2196–2205.
4. VanWeelden K, Flanagan L, Binderup L, Tenniswood M, Welsh J. Apoptotic regression of MCF-7 xenografts in nude mice treated with the vitamin D_3 analog, EB1089. Endocrinology 1998;139:2102–2110.
5. Peng X, Hawthorne M, Vaishnav A, St-Arnaud R, Mehta RG. 25-Hydroxyvitamin D_3 is a natural chemopreventive agent against carcinogen induced precancerous lesions in mouse mammary gland organ culture. Breast Cancer Res Treat 2009;113:31–41.
6. Zinser GM, Welsh J. Vitamin D receptor status alters mammary gland morphology and tumorigenesis in MMTV-neu mice. Carcinogenesis 2004;25:2361–2372.
7. Colston K, Colston MJ, Feldman D. 1,25-Dihydroxyvitamin D_3 and malignant melanoma: the presence of receptors and inhibition of cell growth in culture. Endocrinology 1981;108:1083–1086.
8. Deeb KK, Trump DL, Johnson CS. Vitamin D signalling pathways in cancer: potential for anticancer therapeutics. Nat Rev Cancer 2007;7:684–700.
9. Muindi JR, Peng Y, Potter DM, Hershberger PA, Tauch JS, Capozzoli MJ, Egorin MJ, Johnson CS, Trump DL. Pharmacokinetics of high-dose oral calcitriol: results from a phase 1 trial of calcitriol and paclitaxel. Clin Pharmacol Ther 2002;72:648–659.
10. Muindi JR, Modzelewski RA, Peng Y, Trump DL, Johnson CS. Pharmacokinetics of 1alpha, 25-dihydroxyvitamin D_3 in normal mice after systemic exposure to effective and safe antitumor doses. Oncology 2004;66:62–66.

11. Beer TM, Ryan CW, Venner PM, Petrylak DP, Chatta GS, Ruether JD, Redfern CH, Fehrenbacher L, Saleh MN, Waterhouse DM, Carducci MA, Vicario D, Dreicer R, Higano CS, Ahmann FR, Chi KN, Henner WD, Arroyo A, Clow FW. Double-blinded randomized study of high-dose calcitriol plus docetaxel compared with placebo plus docetaxel in androgen-independent prostate cancer: a report from the ASCENT Investigators. J Clin Oncol 2007;25:669–674.
12. Trump DL, Potter DM, Muindi J, Brufsky A, Johnson CS. Phase II trial of high-dose, intermittent calcitriol (1,25 dihydroxyvitamin D_3) and dexamethasone in androgen-independent prostate cancer. Cancer 2006;106:2136–2142.
13. Carlberg C, Seuter S. A genomic perspective on vitamin D signaling. Anticancer Res 2009;29:3485–3493.
14. Jensen SS, Madsen MW, Lukas J, Binderup L, Bartek J. Inhibitory effects of 1alpha,25-dihydroxyvitamin D(3) on the G(1)-S phase-controlling machinery. Mol Endocrinol 2001;15: 1370–1380.
15. Simboli-Campbell M, Narvaez CJ, van Weelden K, Tenniswood M, Welsh J. Comparative effects of $1,25(OH)_2D_3$ and EB1089 on cell cycle kinetics and apoptosis in MCF-7 breast cancer cells. Breast Cancer Res Treat 1997;42:31–41.
16. Narvaez CJ, Welsh J. Role of mitochondria and caspases in vitamin D-mediated apoptosis of MCF-7 breast cancer cells. J Biol Chem 2001;276:9101–9107.
17. Mathiasen IS, Sergeev IN, Bastholm L, Elling F, Norman AW, Jäättelä MJ. Calcium and calpain as key mediators of apoptosis-like death induced by vitamin D compounds in breast cancer cells. J Biol Chem 2002;277:30738–30745.
18. Swami S, Raghavachari N, Muller UR, Bao YP, Feldman D. Vitamin D growth inhibition of breast cancer cells: gene expression patterns assessed by cDNA microarray. Breast Cancer Res Treat 2003;80:49–62.
19. Towsend K, Trevino V, Falciani F, Stewart PM, Hewison M, Campbell MJ. Identification of VDR-responsive gene signatures in breast cancer cells. Oncology 2006;71:111–123.
20. Ravid A, Koren R. The role of reactive oxygen species in the anticancer activity of vitamin D. Recent Results Cancer Res 2003;164:357–367.
21. Byrne BM, Welsh J. Altered thioredoxin subcellular localization and redox status in MCF-7 cells following 1,25-dihydroxyvitamin D_3 treatment. J Steroid Biochem Mol Biol 2005;97:57–64.
22. Byrne B, Welsh J. Identification of novel mediators of vitamin D signaling and $1,25(OH)_2D_3$ resistance in mammary cells. J Steroid Biochem Mol Biol 2007;103:703–707.
23. Perry RR, Mazetta JA, Levin M, Barranco SC. Glutathione levels and variability in breast tumors and normal tissue. Cancer 1993;72:783–787.
24. Bailey HH. L-S,R-buthionine sulfoximine: historical development and clinical issues. Chem Biol Interact 1998;111–112: 239–254.
25. Lewis-Wambi JS, Swaby R, Kim H, Jordan VC. Potential of L-buthionine sulfoximine to enhance the apoptotic action of estradiol to reverse acquired antihormonal resistance in metastatic breast cancer. J Steroid Biochem Mol Biol 2009;114: 33–39.
26. Lewandowicz GM, Britt P, Elgie AW, Williamson CJ, Coley HM, Hall AG, Sargent JM. Cellular glutathione content, in vitro chemoresponse, and the effect of BSO modulation in samples derived from patients with advanced ovarian cancer. Gynecol Oncol 2002;85:298–304.
27. Marchionatti AM, Picotto G, Narvaez CJ, Welsh J, Tolosa de Talamoni NG. Antiproliferative action of menadione and 1,25(OH)2D3 on breast cancer cells. Steroid Biochem Mol Biol 2009;113:227–232.
28. Bailey HH, Ripple G, Tutsch KD, Arzoomanian RZ, Alberti D, Feierabend C, Mahvi D, Schink J, Pomplun M, Mulcahy RT, Wilding G. Phase I study of continuous-infusion L-S,R-buthionine sulfoximine with intravenous melphalan. J Natl Cancer Inst 1997;89:1789–1796.
29. Hadzic T, Aykin-Burns N, Zhu Y, Coleman MC, Leick K, Jacobson GM, Spitz DR. Paclitaxel combined with inhibitors of glucose and hydroperoxide metabolism enhances breast cancer cell killing via H_2O_2-mediated oxidative stress. Free Radic Biol Med 2010;48:1024–1033.
30. Schnelldorfer T, Gansauge S, Gansauge F, Schlosser S, Beger HG, Nussler AK. Glutathione depletion causes cell growth inhibition and enhanced apoptosis in pancreatic cancer cells. Cancer 2000;89:1440–1447.
31. Rudin M, Yang Z, Schumaker LM, VanderWeele DJ, Newkirk K, Egorin MJ, Zuhowski EG, Cullen KJ. Inhibition of glutathione synthesis reverses Bcl-2-mediated cisplatin resistance. Cancer Res 2003;63:312–318.
32. Elenbaas B, Spirio L, Koerner F, Fleming MD, Zimonjic DB, Donaher JL, Popescu NC, Hahn WC, Weinberg RA. Human breast cancer cells generated by oncogenic transformation of primary mammary epithelial cells. Genes Dev 2001;15:50–65.
33. Burgess A, Vigneron S, Brioudes E, Labbé J-C, Lorca T, Castro A. Loss of human Greatwall results in G2 arrest and multiple mitotic defects due to deregulation of the cyclin B-Cdc2/PP2A balance. Proc Natl Acad Sci USA 2010;107:12564–12569.
34. Darzynkiewicz Z. Cell cycle analysis by flow cytometry. In Handbook of Cell Biology, JE Celis (ed.). San Diego, CA: Academic Press Inc., 1994, 261–271.
35. Anderson M. Determination of glutathione and glutathione disulfide in biological samples. Methods Enzymol 1985;113: 548–555.
36. Bradford MM. A rapid and sensitive method for the quantitation of microgram quantitites of protein utilizing the principle of protein-dye binding. Anal Biochem 1976;72:248–254.
37. Koren R, Ravid A. Vitamin D and the cellular response to oxidative stress. In Vitamin D, 2nd edition, D Feldman, JW Pike, and FH Glorieux (eds.). Burlington, MA, USA: Elsevier Academic Press, 2005, 762–770.
38. Valko M, Rhodes CJ, Moncol J, Izakovic M, Mazur M. Free radicals, metals and antioxidants in oxidative stress-induced cancer. Chem Biol Interact 2006;160:1–40.
39. Marengo B, de Ciucis C, Verzola D, Pistoia V, Raffaghello L, Patriarca S, Balbis E, Traverso N, Cottalasso D, Pronzato MA, Marinari UM, Domenicotti C. Mechanisms of BSO (L-buthionine-S,R-sulfoximine)-induced cytotoxic effects in neuroblastoma. Free Radic Biol Med 2008;44:474–482.
40. Han YH, Park WH. The effects of N-acetyl cysteine, buthionine sulfoximine, diethyldithiocarbamate or 3-amino-1,2,4-triazole on antimycin A-treated Calu-6 lung cells in relation to cell growth, reactive oxygen species and glutathione. Oncol Rep 2009;22:385–391.
41. Chen J, Small-Howard A, Yin A, Berry MJ. The responses of Ht22 cells to oxidative stress induced by buthionine sulfoximine (BSO). BMC Neurosci 2005;6: doi:101186/1471-2202-6-10.
42. Macho A, Hirsch T, Marzo I, Marchetti P, Dallaporta B, Susin SA, Zamzami N, Kroemer G. Glutathione depletion is an early and calcium elevation is a late event of thymocyte apoptosis. J Immunol 1997;158:4612–4619.
43. Syng-Ai C, Kumari AL, Khar A. Effect of curcumin on normal and tumor cells: role of glutathione and bcl-2. Mol Cancer Ther 2004;3:1101–1108.
44. Tsujimoto Y, Shimizu S. Role of the mitochondrial membrane permeability transition in cell death. Apoptosis 2007;12: 835–840.
45. Hildeman DA, Mitchell T, Aronow B, Wojciechowski S, Kappler J, Marrack P. Control of Bcl-2 expression by reactive oxygen species. Proc Natl Acad Sci 2003;100:15035–15040.
46. Kemmis CM, Welsh J. Mammary epithelial cell transformation is associated with deregulation of the vitamin D pathway. J Cell Biochem 2008;105:980–988.

47. O'Dwyer PJ, Hamilton TC, LaCreta FP, Gallo JM, Kilpatrick D, Halbherr T, Brennan J, Bookman MA, Hoffman J, Young RC, Comis RL, Ozols RF. Phase I trial of buthionine sulfoximine in combination with melphalan in patients with cancer. J Clin Oncol 1996;14:249–256.
48. Yao K, Godwin AK, Ozols RF, Hamilton TC, O'Dwyer PJ. Variable baseline γ-glutamylcysteine synthetase messenger RNA expression in peripheral mononuclear cells of cancer patients, and its induction by buthionine sulfoximine treatment. Cancer Res 1993;53:3662–3666.
49. Defty CD, Marsden JR. Melphalan in regional chemotherapy for locally recurrent metastatic melanoma. Current Top Med Chem 2012;12:53–60.
50. Reynolds PC. Chemotherapy in Treating Children with Neuroblastoma. Available at: http://clinicaltrials.gob/ct2/results?term=buthionine+sulfoximine, March 27, 2012.